Journal of Engineering and Technological Sciences

Research Paper

A Cobalt-based Nanostructured Electrode Prepared by a Fast Chemical Method

Nuha A. Alhebshi

Department of Physics, Faculty of Science, Taibah University, Yanbu 46522, Saudi Arabia

*Corresponding author: nalhebshi@taibahu.edu.sa

Abstract

The demand for nanomaterials is rapidly increasing in most applications, such as energy storage devices. Many nanomaterial synthesis methods are energy-consuming methods requiring high temperatures, prolonged reaction time, complicated steps, or expensive equipment. Herein, nanostructures of cobalt hydroxide chloride, $Co_2(OH)_3Cl$, have been directly deposited on carbon cloth microfibers by a fast and simple step of chemical bath deposition. $Co_2(OH)_3Cl$ nanoparticles appear in only 10 minutes of the deposition time, then the nanoflakes are grown in 60 minutes, as imaged by scanning electron microscope. The crystal structure of $Co_2(OH)_3Cl$ is characterized using X-ray diffraction, while the results of energy-dispersive X-ray spectroscopy confirm the elemental analysis. The electrochemical energy storage mechanism of $Co_2(OH)_3Cl$ electrode in potassium hydroxide electrolyte depends on the semi-reversible redox reactions as investigated by the cyclic voltammetry and by the galvanostatic charge-discharge measurements. As a result, the prepared electrode in 60 min exhibits a maximum specific capacitance of 313 F/g versus 293 F/g for the prepared electrode in 10 min, both at 1 A/g. The good electrochemical performance is attributed to several features, including the nanoflakes morphology that enables electrolyte ions to penetrate the electrode freely, the well-crystallized structure, and the solid electronic path between the current collector and the active material indicated by the Nyquist plot of electrochemical impedance spectroscopy. Our cost-effective synthesis of cobalt hydroxide chloride nanostructures on woven substrates offers flexible binder-free electrodes in alkaline electrolytes. This research opens up the potential for these materials to be used as a power source in smart textiles and wearable electronics, thereby contributing to the advancement of these fields.

Keywords: *carbon microfibers; chemical bath deposition; cobalt hydroxide chloride; nanostructures; supercapacitors.*

Introduction

The revolution in nanomaterials science and engineering has been rapidly expanding in diverse fields, including, but not limited to, intelligent textiles, portable electronics, and the Internet of Things. Such advanced applications require improved energy storage devices, such as supercapacitors, with excellent performance, high mechanical flexibility, and cost-effective fabrication (S. Y. Liu et al., 2024; Shaheen et al., 2024; Shalini, Naveen, Durgalakshmi, Balakumar, & Rakkesh, 2024). It has been found that many transition metal oxides/hydroxides and their nanocomposites could be utilized for supercapacitor electrodes (Asghar et al., 2024; Luo, San, Wang, Meng, & Tao, 2024; Malavekar, Pujari, Jang, Bachankar, & Kim, 2024; Meena, Sivasubramaniam, David, & Santhakumar, 2024). Among them, cobalt-based nanomaterials have been considered promising electrode candidates due to their excellent electrochemical properties (Hu, Wang, Wu, & Li, 2021; Pore, Fulari, Shejwal, Fulari, & Lohar, 2021; R. Z. Wu, Sun, Xu, & Chen, 2021; Xu, Yan, Wang, Wang, & Cheng, 2021). They can be synthesized using various methods with functional properties for various applications (Patel, Sereda, & Banerjee, 2021; Yu et al., 2024; Yun et al., 2024; Zhang, Xue, Yan, Gao, & Gao, 2023). However, the most commonly used synthesis methods require high temperatures, long reaction times, and expensive equipment. For example, M. Mansournia and N. Rakhshan prepared $Co_2(OH)_3Cl$ nanoparticles in hydrothermal reaction times of 24 h, 6 h, and 1 h at 100°C using dichlorobis(thiourea)cobalt(II) ethanolic solution ($Co(TU)_2Cl_2$) as a precursor (Mansournia & Rakhshan, 2017). Stick-like and bud-like morphologies of $Co_2(OH)_3Cl$ were obtained by S. Ganguli et al. in 6 hours at 120°C using cobalt(II) chloride hexahydrate in 5:1 of ethanol:water mixture (Ganguli, Koppisetti, Ghosh, Biswas, & Mahalingam, 2019). At the exact temperature of 120°C, nanorods of cobalt hydroxide carbonate were hydrothermally formed in 12 h, 9 h, 6 h, and 3 h by T. Masikhwa and co-researchers (Masikhwa et al., 2016). In another example, the alternating voltage-induced electrochemical method was applied by M. Jing et al. (Jing et al., 2015) to synthesize $Co_2MnO_4/Co_2(OH)_3Cl$ nanocomposite with drying for 12 h at 50°C. This produces a specific capacitance of 779 F/g at 1 A/g in 2 M of a potassium hydroxide (KOH) electrolyte.

ISSN: 2337-5779

J. Eng. Technol. Sci. Vol. 57, No. 2, 2025, 187-195
DOI: 10.5614/j.eng.technol.sci.2025.57.2.4

In all the cases mentioned above, the precipitated materials are powder; hence, a binder is required to fabricate electrodes with current collector substrates. Notably, a nickel foam substrate was straightforwardly coated by nanowires of cobalt chloride carbonate hydroxide deposited in 6 h at 95°C in a water-based solution including $CoCl_2$ and $CO(NH_2)_2$. That binder-free electrode delivers an areal capacitance of 3.48 F/cm^2 at 2.5 mA/cm^2 (1737 F/g at 1.25 A/g) in 1 M KOH, as reported by D. Wu et al. (D. Wu et al., 2016).

Instead of using nickel foam or stainless steel substrates, carbon cloth has attracted attention as a current collector for supercapacitors (X. Q. Liu et al., 2020; Mishra, Shetti, Basu, Reddy, & Aminabhavi, 2019). Carbon cloth microfibers were conformally coated by $Ni(OH)_2$ and Ni-Co-OH nanoflakes using chemical bath deposition for 1-2 h at room temperature, as described in our previous works (Alhebshi & Alshareef, 2015; Alhebshi, Rakhi, & Alshareef, 2013). In the present work, $Co_2(OH)_3Cl$ nanoflakes have been directly deposited on carbon cloth microfibers by chemical bath deposition in only one hour at room temperature. Moreover, the correlation between the material properties and the supercapacitor performance has been investigated.

Experiments

Electrodes Synthesis

Our cobalt-based electrodes were prepared by a simple, fast, and economical chemical bath deposition method directly on a flexible carbon substrate (carbon cloth 7302003, 99% carbon content and 11.5 mg/cm^2, Fuel Cell Store, USA). First, several pieces of the carbon were weighed and vertically attached in two Pyrex beakers. Second, 1.0 M of cobalt(II) chloride hexahydrate ($CoCl_2.6H_2O$) was dissolved in deionized (DI) water in the beakers. Third, 1.56 mL of ammonium hydroxide solution (NH_4OH, 30%-33% NH_3 in H_2O) was drop-by-drop added to the dissolved cobalt salt with stirring at room temperature. An area of 1.0 cm^2 of each carbon piece was immersed into the mixture. After 10 min, the coated carbon substrates were removed from one beaker, and the solution was filtered to collect the residue, while the substrates in the other beaker remained until 60 min. Finally, both sample types, hereafter denoted S-10 min and S-60 min, were washed with DI water and dried in air overnight at room temperature. The mass difference before and after the deposition is considered the mass loading of the active electrode material. It was found between 0.25 mg and 0.50 mg in our samples using a microbalance (XP26 Model, METTLER TOLEDO, USA). In our experiments, the grade of the used chemicals is analytical with no additional purification (Sigma-Aldrich, USA).

Structural Characterization

The molecular formula and the crystal structure of the prepared samples were determined using an X-ray diffraction (XRD) system equipped with a source of CuK, as its wavelength λ is 0.15406 nm (D8 Advance Model, Bruker Corporation, USA). To identify the elements of the electrode materials, energy-dispersive X-ray spectroscopy (EDAX) was applied along with a scanning electron microscope (SEM, Nova Nano 360 Model, FEI Company, USA). Using secondary electron detectors of SEM, which are called Everhart-Thornley detectors (ETD) and through-the-lens detectors (TLD), the morphology of the electrodes was magnified in nanometer and micrometer scales using an electron beam voltage of 5 kV.

Electrochemical Measurements

In a standard three-electrode configuration of the electrochemical workstation (CHI 660D Model, CH Instruments Incorporation USA), our prepared samples were set up as working electrodes, with a reference electrode of saturated calomel electrode (SCE) and a counter electrode of platinum wire. An aqueous electrolyte of 1 M KOH was utilized at room temperature for the following electrochemical tests. Cyclic voltammetry (CV) and galvanostatic charge-discharge (GCD) were conducted to investigate the charge storage mechanism and to calculate the specific (gravimetric) capacitance of the electrodes according to the Eq. (1) (Taberna & Simon, 2013):

$$C_s = (I \Delta t) / (m \Delta V) \quad (1)$$

where I is the applied current of GCD in ampere (A), Δt is the discharge time in second (s), m is the mass loading of the electrode active materials in gram (g), and ΔV is the discharge potential in volt (V). In addition, equivalent series resistance (ESR), charge transfer resistance (R_{CT}), and electrolyte diffusion were pointed out from Nyquist plots of electrochemical impedance spectroscopy (EIS).

DOI: 10.5614/j.eng.technol.sci.2025.57.2.4

Results and Discussion

The XRD spectra of the as-obtained S-10 min and S-60 min powder are analyzed in Figure 1(a). The prominent peaks of our both samples are centered at angels of 16.2°, 32.1°, 39.3°, 50.0°, and 53.6°, which are respectively well-matched with the atomic planes of (101), (113), (024), (033), and (220) in the standard data of rhombohedral crystal $Co_2(OH)_3Cl$ (JCPDS card number of 73-2134) (Ma et al., 2014). The presence of chloride in the resultant instead of pure cobalt hydroxide or oxide is expected since $CoCl_2.6H_2O$ reacts with the OH^- ions at room temperature without an additional oxidizer or post-treatment. It is seen that the diffraction peaks of S-60 min are sharper than those of S-10 min, indicating that the nucleation and growth of $Co_2(OH)_3Cl$ in 60 min produce an improved crystallization. Figure 1 (b) shows the elemental spectrum of the deposited S-60 min thin film, including carbon from the substrate, oxygen, cobalt, chlorine, and negligible aluminum (< 1.0 %). The element weight (Wt%) and corresponding atomic weight (At%) percentages confirm the purity of the sample without foreign elements from the precursors used in the chemical bath deposition.

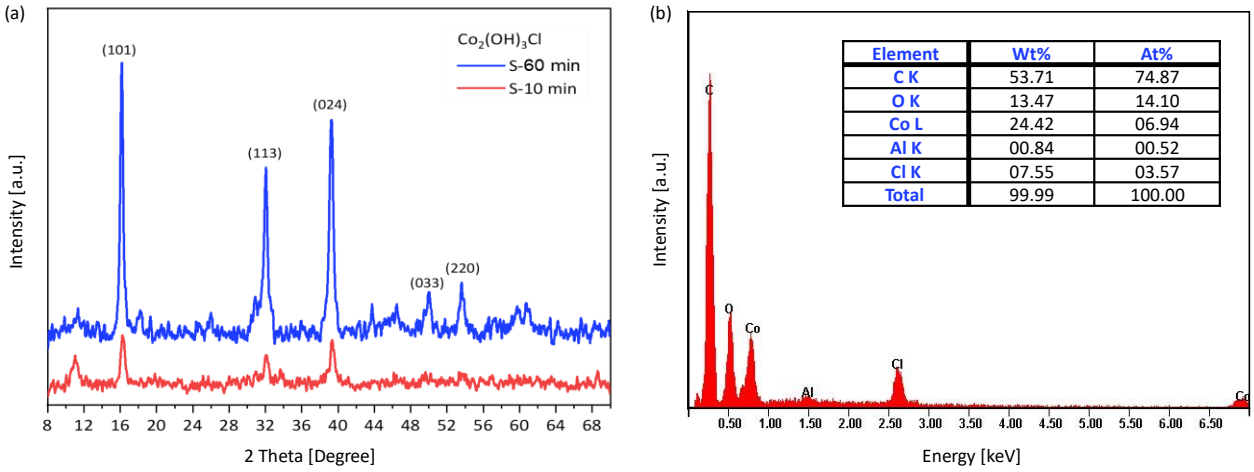

Figure 1 (a) XRD spectra of the as-obtained S-10 min and S-60 min powder, and (b) EDAX spectrum of S-60 min thin film on carbon substrate with its element weight and atomic weight percentages.

The nucleation and growth of $Co_2(OH)_3Cl$ are further monitored using SEM after 10 min and 60 min of the chemical bath deposition. Figure 2 (a-c) displays initial nanoparticles distributed on the microfibers of the carbon substrate. The nanoparticles evolve to vertical nanoflakes in 60 min, as seen in Figure 2 (d-f). The plausible growth mechanisms are initially based on the hydrolyzation of $CoCl_2.6H_2O$ with NH_4OH to produce monomers of cobalt hydroxide hydrate. Then, the monomers precipitate as nuclei that grow up by decomposition of NH_4OH. Increasing the synthesis reaction time can allow further decomposition of NH_4OH, hance building more layers of cobalt hydroxide hydrate. Similar growth mechanisms of nanostructures are reported for carbonated cobalt chloride hydroxide hydrate prepared at different times using a hydrothermal method by Mahmood N. *et. al.* (Mahmood et al., 2015). The $Co_2(OH)_3Cl$ nanostructures are conformally deposited on each carbon microfiber in both samples. This industrial substrate offers flexible 3-dimensional woven fabric that facilitates the passage of the supercapacitor electrolyte through the electrode active materials instead of the 2-dimensional flat substrates such as stainless steel sheets. It is noteworthy that the as-prepared electrodes are binder-free thin films opposite the traditional bulky electrodes that use additional binders to attach the active material powder to the substrates.

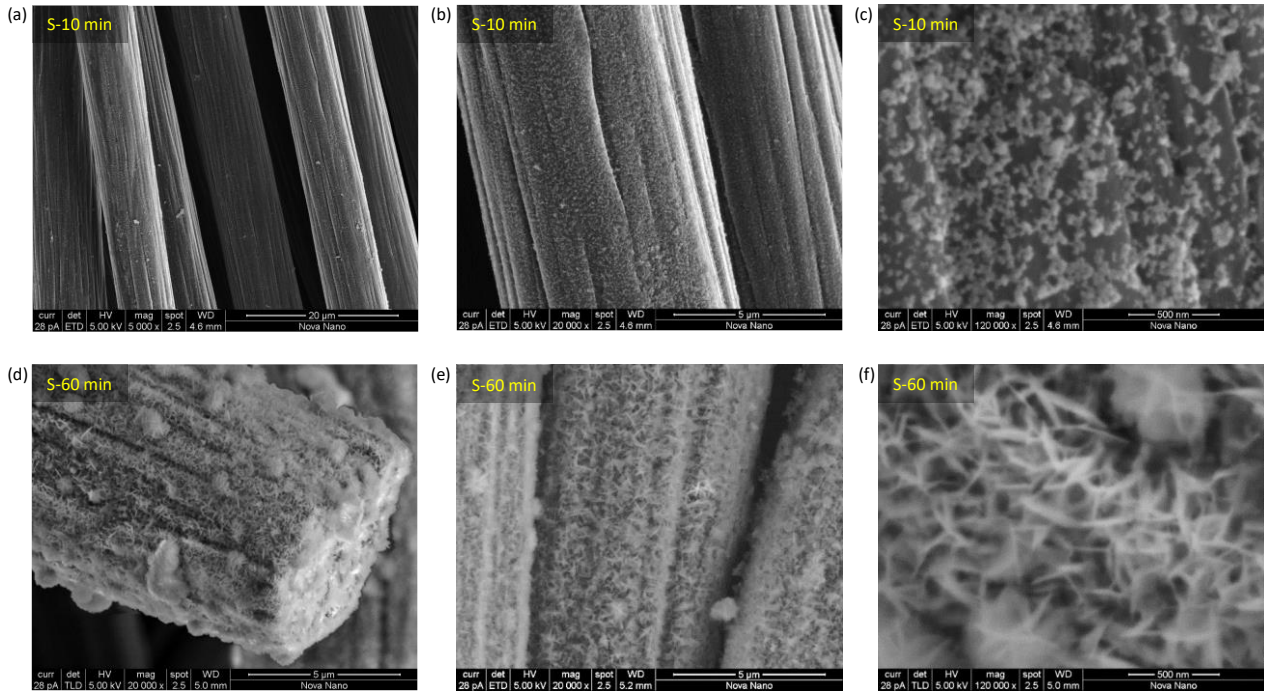

Figure 2 SEM images of $Co_2(OH)_3Cl$ in (a-c) S-10 min nanoparticles and (d-f) S-60 min nanoflakes on carbon microfibers at different magnifications.

Figure 3 (a and b) demonstrate the CV curves of S-60 min and S-10 min electrodes, respectively, in KOH electrolyte at potential scan rates between 100 mV/s and 10 mV/s. The limits of the potential windows are optimized to avoid any oxygen and hydrogen evolution reactions from the aqueous electrolyte. To clarify the current density peaks at 10 mV/s of both samples, the curves are compared in Figure 3 (c). As expected, there are two anodic peaks in the positive current range and two cathodic peaks in the opposing current range, respectively, resulting from the quasi-reversible oxidation and reduction reactions with KOH (Cao, Xu, Liang, & Li, 2004). At 10 mV/s, the peaks in S-60 min at 44 mV and 150 mV are separated by 106 mV, which is a shorter potential distance than 160 mV in S-10 min between 23 mV and 183 mV, pointing out that the redox reactions in S-60 min have better reversibility. At higher scan rates, the potential separations are increased in both samples, and S-60 min still exhibits better reversibility.

The kinetics of the charge-storage mechanism can be qualitatively described based on the exponent value (b) of the power-law Eq. (2):

$$i(v) = a\, v^b \quad (2)$$

where *i* is the peak current, *v* is the scan rate, *a* is a constant, and *b* is the exponent that can be determined by the slope of the linear relation between *log(i)* and *log(v)*. If the *b* value equals 0.5, the mechanism is controlled by the semi-infinite linear diffusion of electrolyte ions into the electrode's layers. In another case, the surface-controlled mechanism occurs when the *b* value equals 1 (Y. Liu, Jiang, & Shao, 2020). As calculated from Figure 3 (d) and represented in the fitting Eqs. (3) and (4), the slops for S-60 min and S-30 min are 0.72 and 0.68, respectively. Such values indicate a combination of slow diffusion and surface-controlled processes.

$$i = 0.72\, v + 0.25 \quad \text{(S-60 min)} \quad (3)$$

$$i = 0.68\, v + 0.21 \quad \text{(S-10 min)} \quad (4)$$

In Figure 3 (e) and Eqs. (5) and (6), it is found that *i* is linearly proportional to $v^{0.5}$ in both samples. The slope in S-60 min is slightly higher than in S-10 min, indicating a better diffusion in S-60 min.

$$i = 1.44\, v^{0.5} + 0.25 \quad \text{(S-60 min)} \quad (5)$$

$$i = 1.37\, v^{0.5} + 0.21 \quad \text{(S-10 min)} \quad (6)$$

The Nyquist plot's slope, nearly 45°, can also confirm the electrolyte ions' diffusion into the electrode at the low-frequency range, as Figure 3 (f) illustrates. At the high-frequency range, the impedance curve approaches the x-axis at

DOI: 10.5614/j.eng.technol.sci.2025.57.2.4

9.6 ohm for S-60 min and 11.9 ohm for S-10 min. These equivalent series resistance (ESR) values include the electrode, substrate, and solution resistances. Besides, the semicircle diameter represents the charge transfer resistance (R_{CT}). The R_{CT} of S-60 min seems to be 2.0 ohm, while no semicircle is found for S-10 min. The reason could be that the increased growth of nanoflakes provides more active sites for charge transfer by the redox reactions in S-60 min. The partially uncoated carbon fibers in S-10 min could decrease the redox contribution of the distributed nanoparticles. It has been reported that such commercial carbon cloth has a low specific capacitance of around 1-2 F/g when used as electrodes without treatment or coating (Chen et al., 2024).

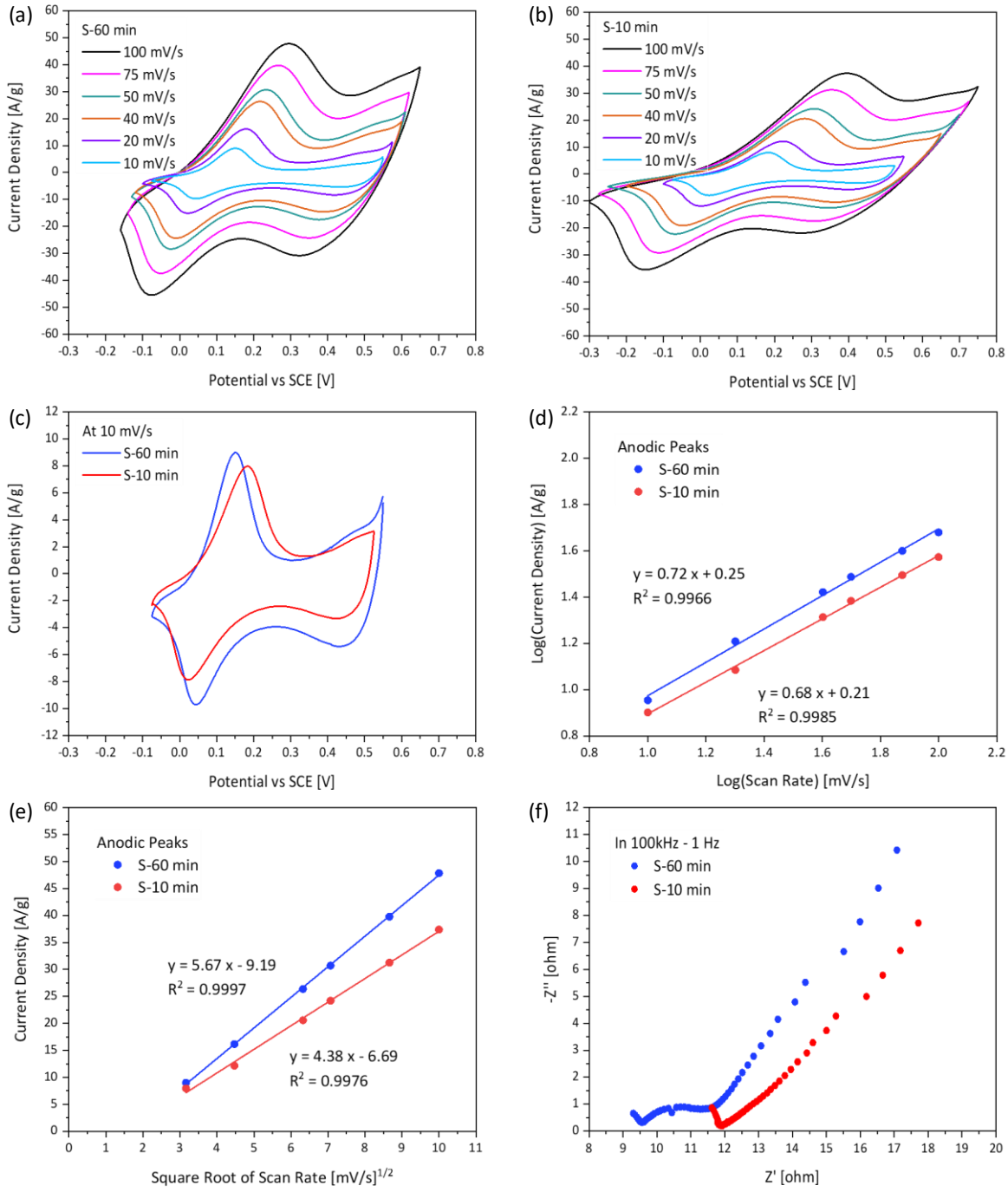

Figure 3 (a and b) CV curves of S-60 min and S-10 min in 1 M KOH, respectively, (c) CV curves of both samples at a scan rate of 10 mV/s, (d and e) the current density of anodic peaks as functions of scan rate and the square root of scan rate, respectively, with linear fitting equations, and (f) Nyquist plot of EIS.

By applying constant anodic and cathodic current densities on the electrodes, the electrical charges are stored and then released in pre-set limits of the potential window, as demonstrated in the GCD curves of Figure 4 (a-e). In analogy with

the CV peaks mentioned above, the GCD reveals two plateaus in all charge curves and other corresponding plateaus in the discharge curves of both $Co_2(OH)_3Cl$ electrodes. It is well-known that supercapacitors are charged and discharged faster by applying high current densities, such as 12 A/g, than low values, such as 1 A/g. Nevertheless, the specific capacitance values, also called gravimetric capacitance, are calculated within a wide range of current density using equation (1), as evaluated in Figure 4 (f). The S-60 min electrode exhibits longer discharge times, hence higher specific capacitances than the S-10 min electrode at all current densities.

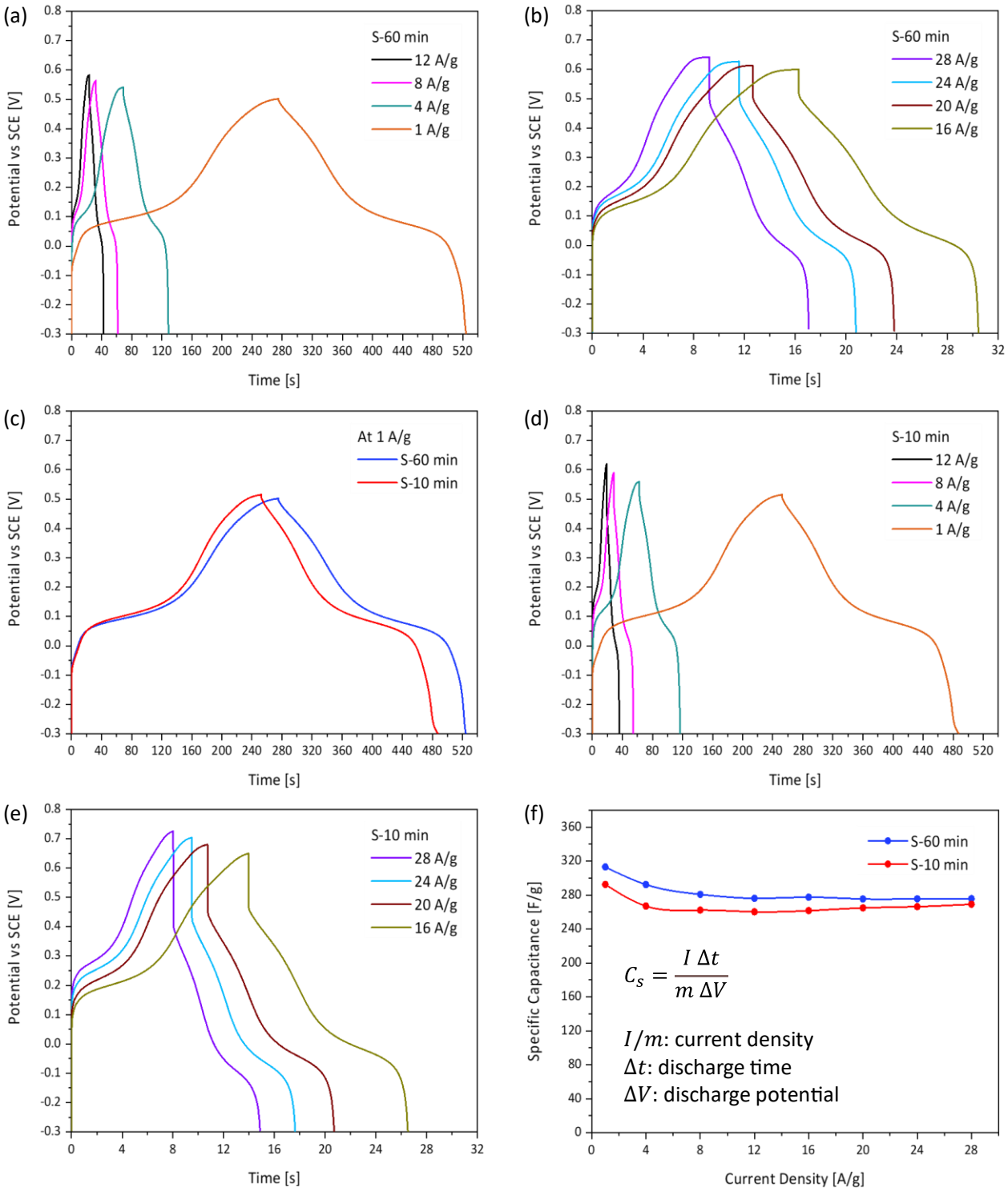

Figure 4 (a and b) GCD curves of S-60 min at low and high current densities, respectively, (c) GCD curves of both samples at a current density of 1 A/g, (d and e) GCD curves of S-10 min at low and high current densities, respectively, and (f) specific capacitance functions of both samples.

DOI: 10.5614/j.eng.technol.sci.2025.57.2.4

An increase in specific capacitance with increasing the synthesis time has been reported in the work of T. Masikhwa and co-researchers (Masikhwa et al., 2016). They concluded that the specific capacitance at 1 A/g of cobalt hydroxide carbonate nanorods in 6 M KOH increases from 208 F/g to 466 F/g by increasing the growth time from 3 h to 12 h. Those long hours led to an increase in the specific surface area of the nanorods. Table 1 lists a comparison of the synthesis time and supercapacitor performance for cobalt-based nanostructured electrodes. Our results of 293 F/g for S-10 min and 313 F/g for S-60 min at 1 A/g are achieved in shorter times than the reported values. The good supercapacitor performance in our work is attributed to many factors, including the growth of nanoflake morphology, which seems to provide a more extensive electrode-electrolyte interface than the nanoparticles of S-10 min. In addition, the better crystallization of $Co_2(OH)_3Cl$ in S-60 min than in S-10 min could support the reversibility of the redox reactions. Both samples' overall electrochemical performance can be ascribed to the conformal coating and firm $Co_2(OH)_3Cl$ attachment on each carbon fiber by the chemical bath deposition. Our binder-free cobalt-based electrodes on fabric substrates have proved promising for flexible supercapacitors. They could find applications as energy storage components in intelligent textiles, portable electronics, and the Internet of Things.

Table 1 A comparison of the synthesis time and supercapacitor performance for cobalt-based nanostructured electrodes.

Electrode	Synthesis Time and Method	Electrolyte	Specific Capacitance at 1 A/g	Reference
Cobalt hydroxide chloride nanosheets	60 minutes in chemical bath deposition	1 M KOH aqueous	313 F/g	This research
Cobalt hydroxide chloride nanoparticles	10 minutes in chemical bath deposition	1 M KOH aqueous	293 F/g	This research
Cobalt hydroxide carbonate nanorods	12 hours in hydrothermal method	6 M KOH aqueous	466 F/g	(Masikhwa et al., 2016)
Cobalt hydroxide carbonate nanorods	3 hours in hydrothermal method	6 M KOH aqueous	208 F/g	(Masikhwa et al., 2016)
Chlorine-doped carbonated cobalt hydroxide nanorods	12 hours in hydrothermal method	1 M KOH aqueous	8808 F/g	(Mahmood et al., 2015).

Conclusion

A simple, fast, and economical chemical bath deposition method has been optimized to produce a conformal $Co_2(OH)_3Cl$ nanostructured coating on carbon microfibers. Interestingly, $Co_2(OH)_3Cl$ nanoparticles appear in only 10 minutes of the deposition time; then, the nanoflakes are grown in 60 minutes. In both cases, the as-prepared $Co_2(OH)_3Cl$ has a rhombohedral crystal structure without a significant atomic weight percentage of impurities. The CV and GCD curves prove that the electrochemical energy storage mechanism of $Co_2(OH)_3Cl$ electrodes in KOH electrolyte depends on semi-reversible redox reactions at the surface and the semi-infinite diffusion process. As a result, the S-60 min exhibits a specific capacitance of 313 F/g at a current density of 1 A/g, higher than 293 F/g at 1 A/g for the S-10 min. The improved performance is achieved because the better crystallinity of S-60 min with nanoflake morphology enables electrolyte ions to penetrate the electrode more efficiently than the nanoparticles. Our optimized synthesis of cobalt hydroxide chloride nanostructures on woven substrates offers binder-free electrodes for flexible supercapacitor applications. It is recommended that further development be made in terms of mechanical flexibility, cyclic stability, and electrical conductivity.

Acknowledgment

The author thanks King Abdullah University of Science and Technology (KAUST) in Saudi Arabia for its laboratory services and Taibah University in Saudi Arabia.

Compliance with ethics guidelines

The authors declare that they have no conflict of interest or financial conflicts to disclose.

This article does not contain any studies with human or animal subjects performed by any of the authors.

References

Alhebshi, N. A., & Alshareef, H. N. (2015). Ternary Ni-Cu-OH and Ni-Co-OH electrodes for electrochemical energy storage. *Materials for Renewable and Sustainable Energy, 4*, 21, 1–9. https://doi.org/10.1007/s40243-015-0064-7

Alhebshi, N. A., Rakhi, R. B., & Alshareef, H. N. (2013). Conformal coating of $Ni(OH)_2$ nanoflakes on carbon fibers by chemical bath deposition for efficient supercapacitor electrodes. *Journal of Materials Chemistry A, 1*(47), 14897–14903. https://doi.org/10.1039/c3ta12936e

Asghar, A., Khan, K., Hakami, O., Alamier, W. M., Ali, S. K., Zelai, T., . . . Al-Harthi, E. A. (2024). Recent progress in metal oxide-based electrode materials for safe and sustainable variants of supercapacitors. *Frontiers in Chemistry, 12,* 1402563. https://doi.org/10.3389/fchem.2024.1402563

Cao, L., Xu, F., Liang, Y. Y., & Li, H. L. (2004). Preparation of the novel nanocomposite $Co(OH)_2$/ultra-stable Y zeolite and its application as a supercapacitor with high energy density. *Advanced Materials, 16*(20), 1853–1857. https://doi.org/ 10.1002/adma.200400183

Chen, M., Zhou, F., Wan, B., Tu, L., Rang, Y., Mao, B., . . . Li, L. (2024). Polypyrrole-assisted surface-oxidized carbon cloth for high-performance flexible solid-state supercapacitors. *Journal of Energy Storage, 99*, 113198. https://doi.org/10.1016/j.est.2024.113198

Ganguli, S., Koppisetti, H., Ghosh, S., Biswas, T., & Mahalingam, V. (2019). Paradoxical Observance of "Intrinsic" and "Geometric" Oxygen Evolution Electrocatalysis in Phase-Tuned Cobalt Oxide/Hydroxide Nanoparticles. *ACS Applied Nano Materials, 2(*12), 7957–7968. https://doi.org/10.1021/acsanm.9b01990

Hu, X. R., Wang, Y., Wu, Q. S., & Li, J. F. (2021). Review of cobalt-based nanocomposites as electrode for supercapacitor application. *Ionics, 27*(11), 4573-4618. doi:10.1007/s11581-021-04319-z

Jing, M., Hou, H., Yang, Y., Zhu, Y., Wu, Z., & Ji, X. (2015). Electrochemically alternating voltage tuned Co_2MnO_4/Co hydroxide chloride for an asymmetric supercapacitor. *Electrochimica Acta, 165*, 198–205. https://doi.org/10.1016/j.electacta.2015.03.032

Liu, S. Y., Yang, J., Chen, P., Wang, M., He, S. J., Wang, L., & Qiu, J. S. (2024). Flexible Electrodes for Aqueous Hybrid Supercapacitors: Recent Advances and Future Prospects. *Electrochemical Energy Reviews, 7*(1), 25. https://doi.org/10.1007/s41918-024-00222-z

Liu, X. Q., Xu, W., Zheng, D. Z., Li, Z. F., Zeng, Y. X., & Lu, X. H. (2020). Carbon cloth as an advanced electrode material for supercapacitors: progress and challenges. *Journal of Materials Chemistry A, 8*(35), 17938-17950. https://doi.org/10.1039/d0ta03463k

Liu, Y., Jiang, S. P., & Shao, Z. (2020). Intercalation pseudocapacitance in electrochemical energy storage: recent advances in fundamental understanding and materials development. *Materials Today Advances, 7*, 100072. https://doi.org/10.1016/j.mtadv.2020.100072

Luo, F. J., San, X. G., Wang, Y. S., Meng, D., & Tao, K. (2024). Layered double hydroxide-based electrode materials derived from metal-organic frameworks: synthesis and applications in supercapacitors. *Dalton Transactions, 53*(25), 10403–10415. https://doi.org/10.1039/d4dt01344a

Ma, J., Yuan, T., He, Y.-S., Wang, J., Zhang, W., Yang, D., . . . Ma, Z.-F. (2014). A novel graphene sheet-wrapped $Co_2(OH)_3Cl$ composite as a long-life anode material for lithium ion batteries. *Journal of Materials Chemistry A, 2*(40), 16925–16930. https://doi.org/10.1039/C4TA03857F

Mahmood, N., Tahir, M., Mahmood, A., Zhu, J., Cao, C., & Hou, Y. (2015). Chlorine-doped carbonated cobalt hydroxide for supercapacitors with enormously high pseudocapacitive performance and energy density. *Nano Energy, 11*, 267–276. https://doi.org/10.1016/j.nanoen.2014.11.015

Malavekar, D., Pujari, S., Jang, S., Bachankar, S., & Kim, J. H. (2024). Recent Development on Transition Metal Oxides-Based Core-Shell Structures for Boosted Energy Density Supercapacitors. *Small, 20*(31), 2312179. https://doi.org/10.1002/smll.202312179

Mansournia, M., & Rakhshan, N. (2017). Hydrothermal synthesis and tuning of size and morphology of α-Co(OH)2 and α-Co2(OH)3Cl nanostructures as precursors for nanosized Co_3O_4. *Ceramics International, 43*(9), 7282-7289. https://doi.org/10.1016/j.ceramint.2017.03.025

Masikhwa, T. M., Dangbegnon, J. K., Bello, A., Madito, M. J., Momodu, D., Barzegar, F., & Manyala, N. (2016). Effect of growth time of hydrothermally grown cobalt hydroxide carbonate on its supercapacitive performance. *Journal of Physics and Chemistry of Solids, 94*, 17–24. https://doi.org/10.1016/j.jpcs.2016.03.004

Meena, J., Sivasubramaniam, S. S., David, E., & Santhakumar, K. (2024). Green supercapacitors: review and perspectives on sustainable template-free synthesis of metal and metal oxide nanoparticles. *RSC Sustainability, 2*(5), 1224–1245. https://doi.org/10.1039/d4su00009a

Mishra, A., Shetti, N. P., Basu, S., Reddy, K. R., & Aminabhavi, T. M. (2019). Carbon Cloth-based Hybrid Materials as Flexible Electrochemical Supercapacitors. *ChemElectroChem, 6*(23), 5771–5786. https://doi.org/10.1002/celc.201901122

DOI: 10.5614/j.eng.technol.sci.2025.57.2.4

Patel, A. R., Sereda, G., & Banerjee, S. (2021). Synthesis, Characterization and Applications of Spinel Cobaltite Nanomaterials. *Current Pharmaceutical Biotechnology, 22*(6), 763–782. https://doi.org/10.2174/1389201021666201117122002

Pore, O. C., Fulari, A. V., Shejwal, R. V., Fulari, V. J., & Lohar, G. M. (2021). Review on recent progress in hydrothermally synthesized MCo_2O_4/rGO composite for energy storage devices. *Chemical Engineering Journal, 426*, 32. https://doi.org/10.1016/j.cej.2021.131544

Shaheen, I., Akkinepally, B., Hussain, I., Hussain, S., Rosaiah, P., Qureshi, A., & Niazi, J. H. (2024). Fabrication of MXene/cellulose composite-based flexible supercapacitor: Synthesis, properties, and future perspectives. *Journal of Energy Storage, 87*, 111513. https://doi.org/10.1016/j.est.2024.111513

Shalini, S., Naveen, T. B., Durgalakshmi, D., Balakumar, S., & Rakkesh, R. A. (2024). Progress in flexible supercapacitors for wearable electronics using graphene-based organic frameworks. *Journal of Energy Storage, 86*, 111260. https://doi.org/10.1016/j.est.2024.111260

Taberna, P.-L., & Simon, P. (2013). Electrochemical Techniques. In Supercapacitors (pp. 111–130).

Wu, D., Xiao, T., Tan, X., Xiang, P., Jiang, L., Kang, Z., & Tan, P. (2016). High-performance asymmetric supercapacitors based on cobalt chloride carbonate hydroxide nanowire arrays and activated carbon. *Electrochimica Acta, 198*, 1–9. https://doi.org/10.1016/j.electacta.2016.01.194

Wu, R. Z., Sun, J. L., Xu, C. J., & Chen, H. Y. (2021). $MgCo_2O_4$-based electrode materials for electrochemical energy storage and conversion: a comprehensive review. *Sustainable Energy & Fuels, 5*(19), 4807–4829. doi:10.1039/d1se00909e

Xu, J. M., Yan, A. L., Wang, X. C., Wang, B. Q., & Cheng, J. P. (2021). A review of cobalt monoxide and its composites for supercapacitors. *Ceramics International, 47*(16), 22229–22239. https://doi.org/10.1016/j.ceramint.2021.04.262

Yu, T. T., Li, S. B., Li, F. B., Zhang, L., Wang, Y. P., & Sun, J. Y. (2024). In-situ synthesized and induced vertical growth of cobalt vanadium layered double hydroxide on few-layered V_2CT_x MXene for high energy density supercapacitors. *Journal of Colloid and Interface Science, 661*, 460–471. https://doi.org/10.1016/j.jcis.2024.01.206

Yun, T. H., Kim, T., Hwang, Y., Velhal, N. B., Park, H. W., Yim, C., & Kim, J. (2024). Laser-Assisted Rapid Fabrication of Cobalt Hydroxide@Carbon Fiber Composites for High-Performance, Robust Structural Supercapacitors. *ACS Applied Energy Materials, 7(*21), 10120–10133. https://doi.org/10.1021/acsaem.4c02261

Zhang, Y., Xue, S. C., Yan, X. H., Gao, H. L., & Gao, K. Z. (2023). Preparation and electrochemical properties of cobalt aluminum layered double hydroxide/carbon-based integrated composite electrode materials for supercapacitors. *Electrochimica Acta, 442,* 141822. https://doi.org/10.1016/j.electacta.2023.141822

Manuscript Received: 10 June 2024
1st Manuscript Revision Received: 4 December 2024
2nd Manuscript Revision Received: 14 January 2025
Accepted Manuscript: 15 January 2025